The Stoichiometry of Subunit *c* of *Escherichia coli* ATP Synthase Is Independent of Its Rate of Synthesis[†]

Thomas Krebstakies,[‡] Ingo Aldag,[‡] Karlheinz Altendorf, Jörg-Christian Greie, and Gabriele Deckers-Hebestreit*

Abteilung Mikrobiologie, Fachbereich Biologie/Chemie, Universität Osnabrück, D-49069 Osnabrück, Germany

Received January 30, 2008; Revised Manuscript Received May 9, 2008

ABSTRACT: Immunoblot quantitation of *Escherichia coli* ATP synthase isolated from *atp* wildtype and mutant cells, the latter comprising a reduced expression of the *atpE* gene coding for subunit *c* due to a point mutation within its Shine−Dalgarno sequence, suggested a variable stoichiometry of subunit *c* [Schemidt et al. (1995) *Arch. Biochem. Biophys. 323*, 423−428]. To study the *c* ring of the mutant strain and its stoichiometry in more detail, F_O isolated from wildtype and mutant were investigated by quantitation, reconstitution, and cross-linking. Direct quantitation by staining with SYPRO Ruby revealed a reduction of subunit *c* in the mutant by a factor of 2 compared to F_O subunits *a* and *b*. Rates of passive H^+ translocation correlated with the amount of subunit *c* present. Lower rates for mutant F_O could be increased by addition of subunit *c*, whereas translocation rates remained constant by coreconstitution with nonfunctional subunit *c*D61G arguing against the presence of smaller *c* rings that are filled up with coreconstituted subunit *c*. Intermolecular cross-linking by oxidation of bicysteine-substituted subunit *c* (*c*A21C/*c*M65C) revealed an equal pattern of oligomer formation in wildtype and mutant also favoring a comparable subunit *c* stoichiometry. Cross-linking of membrane vesicles containing cysteine-substituted subunits *a* (*a*N214C) and *c* (*c*M65C) characterized the mutant F_O preparation as a heterogeneous population, which consists of assembled F_O and free ab_2 subcomplexes each present to approximately 50%. Thus, these data clearly demonstrate that the stoichiometry of the subunit *c* rings remains constant even after reduction of the synthesis of subunit *c*.

In mitochondria, chloroplasts, or eubacteria, ATP synthases catalyze the synthesis of ATP from ADP and inorganic phosphate, utilizing the energy of an electrochemical ion gradient ($\Delta\mu_{H^+}$ or $\Delta\mu_{Na^+}$) generated across the membrane by respiration or photosynthesis. In bacteria, ATP synthases can also serve as primary ion pumps in case of low driving force, thereby generating an ion gradient across the membrane at the expense of ATP. In *Escherichia coli*, the ATP synthase is built up of the membrane complex F_O (ab_2c_{10}), which couples ion translocation to ATP synthesis/hydrolysis within the peripheral catalytic part F_1 ($\alpha_3\beta_3\gamma\delta\varepsilon$) via a rotary mechanism (*1–4*).

Within the F_O complex, subunits *a* and *b* are located outside the ring-like *c* oligomer. Rotation of the *c* ring is driven by the proton motive force. In direction of ATP synthesis, the essential carboxylate *c*D61 in the middle of the C-terminal transmembrane helix of subunit *c* is accessible for protons from the periplasmic side of the membrane via a half-channel within subunit *a*. The binding sites of the oligomeric *c* ring are loaded successively, thereby driving the rotation of the ring relative to the ab_2 stator interface toward the lipid phase of the membrane. After a full rotation of the *c* ring, protons are released to the cytoplasmic side of the membrane due to electrostatic interactions between *a*R210 and *c*D61 through an exit half-channel of subunit *a*. During coupled catalysis, this rotary movement is transferred to the catalytic sites via the centrally located $\gamma\varepsilon$ subcomplex, which is fixed to a set of *c* subunits within the proteolipid ring (*1–4*). Thus, the number of subunit *c* monomers determines the number of transported ions per revolution, which, in turn, directly defines the proton to ATP ratio as well as the P/O ratio of oxidative phosphorylation (compare ref *5*).

F_O complexes from different organisms comprise individual numbers of *c* subunits: ten monomers in the mitochondrial ATP synthase of *Saccharomyces cerevisiae* as well as in the thermophilic *Bacillus* PS3, eleven *c* subunits in the Na^+-translocating ATP synthase of *Ilyobacter tartaricus*, *Propionigenium modestum*, and *Clostridium paradoxum*, 12 copies in the prokaryotic V-ATPase of *Thermus thermophilus*, 14 copies within the *c* oligomers of spinach chloroplasts, and 13−15 *c* subunits in the ATP synthases of different cyanobacteria (compare refs *3, 6–8). In addition, for the A-type ATP synthase of Methanopyrus kandleri, a monomeric proteolipid comprising 13 hairpin domains has been deduced from its sequence (9). A structural analysis of proteolipid rings from I. tartaricus, P. modestum, and spinach chloroplasts furthermore suggested a rather rigid oligomeric structure with an invariant stoichiometry (10, 11). However, in the case of E. coli ATP synthase, the stoichiometry can be experimentally varied by atpE gene fusions resulting in 9−12 c subunits within the ring (12, 13), although the*

[†] Supported by the Deutsche Forschungsgemeinschaft (SFB 431/P2) and by the Fonds der Chemischen Industrie (fellowship to T.K.).

* To whom correspondence should be addressed. Tel: +49-541-9692809. Fax: +49-541-9692870. E-mail: deckers-hebestreit@biologie.uni-osnabrueck.de.

[‡] Both authors contributed equally to this work.

10.1021/bi800173a CCC: $40.75
Published on Web 06/10/2008

Table 1: *E. coli* Strains and Plasmids[a]

E. coli strains/plasmids	genotype/description	ref
DK8	*Hfr*PO1, *bglR*, *thi1*, *relA1*, *ilv::Tn*10, Δ*atpBEFHAGDC*	*23*
LE392Δ*atpI-C* (formerly LE392Δ*uncI-C*)	F$^-$, *supF58*, *supE44*, *hsdR514*, *galK2*, *galT22*, *metB1*, *lacY1, trpR55,* Δ*atpIBEFHAGDC*	*25*
MO202	F$^+$, *thi1*, *relA*, Δ*atpBEFHAGDC*	*22*
MEG132	MO202/pMEG112	R. H. Fillingame
pWSB30.0	Cm^R, *atpI′BEFHAGDC*	*26*
pRPG54	pWSB30.0: point mutation in S/D box of *atpE*	*19*
pBWU13	Ap^R, *atpI′BEFHAGDC*	*20*
pIA1	pBWU13: point mutation in S/D box of *atpE*	this study
pDF163.aN214C/cM65C	Ap^R, *atpBEFH*, *a*N214C, *c*M65C	*21*
pPJC1-21/65	pNOC: *c*A21C, *c*M65C, *b*C21S	*12*
pBWU13.NOC	pBWU13: *c*A21C, *c*M65C, *b*C21S	this study
pRPG54.NOC	pRPG54: *c*A21C, *c*M65C, *b*C21S	this study
pIA1.NOC	pIA1: *c*A21C, *c*M65C, *b*C21S	this study
pIA1.1	pIA1: *c*M65C	this study
pTOM5.0	pBWU13: *a*N214C, *c*M65C	this study
pTOM5.1	pIA1: *a*N214C, *c*M65C	this study
pMEG112	Ap^R, *atpB′EF′*, *c*D61G	R. H. Fillingame

[a] Plasmid pWSB30.0 and derivatives originated from pACYC184, pBWU13 as well as pDF163 and their derivatives emerged from pBR322, and plasmid pMEG112 derived from pUC18.

preferred number of c subunits was revealed to be 10 (13). In addition, studies on the expression of atp genes using LacZ as reporter argue in favor of the notion that the subunit c stoichiometry is variable within one organism depending on the growth conditions (14). This opens the possibility to respond to different metabolic states of the cell, thereby changing the P/O ratio via a regulated subunit c stoichiometry (compare ref 15).

In the case of a point mutation within the S/D box[1] of the *atpE* gene (GGAGA→GGAAA), *E. coli* cells bearing the corresponding plasmid are reported to comprise a 2−3-fold reduced synthesis of subunit *c* (*16, 17*). This spontaneous mutation was obviously obtained as a consequence of overexpression of the *atp* operon, since the resulting mutant showed significantly less membrane proton permeability compared to cells carrying a plasmid with the wildtype *atp* operon (*17*), possibly due to a less dense protein packing within the membrane. This mutation provided a first hint for a putative regulatory mechanism of subunit *c* stoichiometry, which is based on the level of protein synthesis (*18*), since the observed phenotype strongly reflected the results obtained by the reporter gene analysis used for investigation of the subunit *c* stoichiometry in different growth media (*14*).

In order to investigate the possible variability of the subunit *c* stoichiometry in the *E. coli* mutant strain carrying the corresponding G→A transition within the S/D box of the *atpE* gene (*18*) in more detail, F_O preparations from wildtype and mutant cells were studied with respect to both functional and structural aspects. The data obtained by combining rates of passive H^+ translocation of reconstituted F_O with cross-linking experiments in both membrane vesicles and proteoliposomes clearly demonstrated that the subunit *c* stoichiometry in *E. coli* is independent of the rate of subunit *c* synthesis and, thereby, not regulated at the level of mRNA translation. The stoichiometry of the subunit *c* ring is comparable in wildtype and mutant F_O, whereas free ab_2 subcomplexes are present together with fully assembled F_O complexes in mutant F_O preparations each with a rate of approximately 50% resulting together in a reduction of subunit *c* by about a factor of 2 compared to F_O subunits *a* and *b*.

[1] Abbreviations: 2-ME, 2-mercaptoethanol; AFM, atomic force microscopy; DCCD, *N*,*N*′-dicyclohexylcarbodiimide; DTT, dithiothreitol; mAb, monoclonal antibody; S/D box, Shine−Dalgarno sequence.

EXPERIMENTAL PROCEDURES

Bacterial Strains, Plasmids, and Growth Conditions. E. coli strains and plasmids used are described in Table 1. A 2084-bp *Pfl*MI/*Sph*I fragment from pRPG54 (*19*) was ligated into the 8671-bp *Pfl*MI/*Sph*I-digested vector pBWU13 (*20*), yielding plasmid pIA1. Ligation of a 2351-bp *Hin*dIII/*Sph*I fragment from pPJC1-21/65 (*12*) into the 8404-bp *Hin*dIII/*Sph*I-digested vector pBWU13 generated plasmid pBWU13.NOC. A 1290-bp *Bsr*GI/*Afl*II fragment from pPJC1-21/65 was subcloned into the 11911-bp *Bsr*GI/*Afl*II-digested vector pRPG54 to generate pRPG54.NOC, from which a 2084-bp *Pfl*MI/*Sph*I fragment was then ligated into *Pfl*MI/*Sph*I-digested vector pBWU13 to generate plasmid pIA1.NOC.

The 1206-bp *Pfl*MI/*Ppu*MI fragment of pDF163.*a*N214C/*c*M65C (*21*) was ligated into the *Pfl*MI/*Ppu*MI-digested vector pBWU13 to generate pTOM5.0. A 617-bp *Bam*HI fragment of pDF163.*a*N214C/*c*M65C was ligated into the *Bam*HI-digested vector pIA1.1, which was generated by ligation of a 10324-bp *Bsr*GI/*Ppu*MI fragment obtained by partial digestion of pIA1 with a 431-bp *Bsr*GI/*Ppu*MI fragment of pDF163.*a*N214C/*c*M65C, finally yielding plasmid pTOM5.1. Strain MEG132 (kindly provided by Dr. R. H. Fillingame) consists of strain MO202 (*22*) transformed with pMEG112 coding for subunit cD61G.

E. coli strain DK8 (*23*) transformed with plasmid pBWU13 or its derivatives was grown on minimal medium supplemented with thiamin (2 μg/mL), thymine, asparagine, isoleucine, and valine (50 μg/mL each) together with 0.5% (v/v) glycerol as carbon source (*24*). *E. coli* strain LE392Δ*atpI-C* (*25*) transformed with plasmids pWSB30.0 (*26*) or pRPG54 (*19*) was grown on Luria−Bertani rich medium with 50 μg/mL chloramphenicol (*24*). *E. coli* strain MEG132 was grown on M63 minimal medium with 0.2% (w/v) glucose and 100 μg/mL ampicillin supplemented with 1 g/L tryptone, 0.5 g/L yeast extract, and 17 mM NaCl as described (*27*).

To study the influence of the point mutation in the ribosome binding site of *atpE* on the synthesis of the subunits of the ATP synthase with special emphasis on the stoichiometry of subunit *c*, two different expression systems were applied. On the one hand, strain LE392Δ*atpI-C* bearing plasmid pWSB30.0 (wild-type) or pRPG54 (mutation in the S/D box of *atpE*) based on vector pACYC184 (*19, 26*) was used, which has also been utilized in previous work (*17, 18*). However, the wildtype LE392Δ*atpI*-C/pWSB30.0 does not grow on minimal medium with succinate as sole carbon and energy source possibly due to an increased membrane proton permeability (*17*). In addition, strain DK8 transformed with plasmid pBWU13 (wildtype) or pIA1 (mutant) was applied, which is based on vector pBR322 with the *rom* gene deleted (*20*). With this system, growth on minimal medium in the presence of succinate could be observed within 2 days for both constructs (data not shown). Furthermore, transformation of strain DK8 with plasmids pWSB30.0 or pRPG54 also allowed complementation of the chromosomal *atpB-C* deletion by the plasmid-encoded *atp* operon (data not shown). However, F_O preparations with higher yield were consistently obtained by use of strain DK8 transformed with pBWU13 derivatives.

Preparative Procedures. Preparation of F_O and F_1 was carried out as described (*24*). Everted membrane vesicles from DK8/pBWU13.NOC and DK8/pIA1.NOC were prepared using TMG buffer (50 mM Tris-HCl, pH 7.5, 5 mM $MgSO_4$, 10% (v/v) glycerol) (*28*). In the case of DK8/pTOM5.0 and DK8/pTOM5.1, preparation of F_1-depleted membrane vesicles was carried out as described (*29*), with a final resuspension of membranes in TMG buffer. Subunit *c* from *E. coli* strains DK8/pBWU13 (*c*D61) and MEG132 (*c*D61G) was purified by the chloroform/methanol/H_2O procedure (*24*) or by detergent solubilization according to Schneider and Altendorf (*30*).

Reconstitution of F_O into Liposomes. Reconstitution of F_O prepared from LE392Δ*atpI-C*/pWSB30.0 and LE392Δ*atpI-C*/pRPG54 and coreconstitution with detergent-purified subunit *c*D61 were carried out by dialysis (*24*), thereby using a protein-to-phospholipid ratio of 1:133 with phosphatidylcholine type IV-S (Sigma) suspended at 40 mg/mL in detergent buffer. For coreconstitution, stoichiometric amounts of detergent-solubilized subunit *c*D61 were added prior to dialysis. In the case of Mut-F_O[2] and WT-F_O prepared from *E. coli* DK8 bearing pBWU13 derivatives, F_O was coreconstituted with chloroform/methanol/H_2O-purified subunit *c*, either *c*D61 or *c*D61G, according to ref *31* with the following modifications. Preformed liposomes were prepared from *E. coli* lipids (25 mg/ml) (Avanti Pro Lipids) as described by Stalz et al. (*24*). Liposomes with and without subunit *c* were mixed in ratios yielding a 1- or 5-fold stoichiometric excess of subunit *c*, assuming an F_O stoichiometry of ab_2c_{10}. Isolated F_O was added at a protein-to-lipid ratio of 1:208 and 1:104 for WT-F_O and Mut-F_O, respectively, and the Triton X-100 used for "onset solubilization" of preformed liposomes was removed by the subsequent addition of increasing amounts of Bio-Beads SM-2 (Bio-Rad).

Cross-Linking Analyses. Cross-linking studies of membrane vesicles from strains DK8/pBWU13.NOC and DK8/pIA1.NOC were carried out as described (*32*) using 3 mM copper-1,10-phenanthroline. For cross-linking analysis of proteoliposomes, WT-F_O and Mut-F_O prepared from DK8/pBWU13.NOC and DK8/pIA1.NOC, respectively, were reconstituted as described above with a protein-to-lipid ratio of 1:104 and 1:35, respectively. During the reconstitution procedure, 10 mM DTT was added to each sample. After subsequent extrusion (400 nm pore size filter devices), DTT was removed by dialysis against 100 mM potassium phosphate, pH 7.0, for 24 h at 4 °C, changing the buffer twice. Cross-linking was induced by air oxidation, incubating the samples at room temperature overnight after an additional extrusion of the proteoliposomes. The reaction was stopped by addition of an equal volume of SDS−PAGE sample loading buffer without 2-ME (*33*).

Disulfide bond formation between *a*N214C and *c*M65C was induced by air oxidation in the presence of $CuCl_2$ as described (*34*). One mg/mL of F_1-depleted membrane vesicles (DK8/pTOM5.0 or DK8/pTOM5.1) was dialyzed twice against a 1000-fold volume of 50 mM Tris-HCl, pH 8.0, 1 mM EDTA, and 1 mM DTT at 4 °C overnight and then dialyzed against 100 mM Tris-HCl, pH 7.5, 100 mM NaCl, and 50 μM $CuCl_2$.

Densitometric Quantitation of Subunits a, b, and c. Different amounts of isolated WT-F_O and Mut-F_O were separated by SDS−PAGE and stained with SYPRO Ruby as recommended by the supplier (Bio-Rad). For quantitation, the intensities of the bands of subunits *a*, *b*, and *c* were scanned with a Fluor-S MultiImager (Bio-Rad) and analyzed by the QuantityOne software (Bio-Rad). The amount of protein analyzed was adjusted to give a linear correlation between the fluorescent band intensity and the amount of protein applied using the corresponding slope for calculation of the relative amount of every F_O subunit present.

Immunoblotting of cross-linked membrane vesicles and proteoliposomes was performed according to Birkenhäger et al. (*28*) using 10 mM $NaHCO_3$, 3 mM Na_2CO_3, and 20% (v/v) methanol as transfer buffer and mAb GDH 8-8B3 as well as mAb GDH 9-2A2 (for the detection of subunits *a* and *c*, respectively). Blot membranes were incubated with corresponding primary mAbs, horseradish peroxidase-conjugated sheep anti-mouse IgG (diluted 1:10000; Amersham Biosciences), and finally developed on ECL Hyperfilm (Amersham Biosciences) by use of SuperSignal (Pierce). Quantitation of band intensities was performed with the LabImage 2.7.1 software (LabImage) after scanning the film.

Assays. Protein concentrations were determined with either the BCA assay used as recommended by the supplier (Pierce) or according to Dulley and Grieve (*35*). Thereby, different results in protein content on the membrane level were determined, which were generally reflected by 1.6-fold higher protein concentrations determined by the method of Dulley and Grieve (*35*) (data not shown). Proteins were dissolved in SDS−PAGE sample loading buffer (*33*), separated by SDS−PAGE using 16.5% T/6% C separating gels together with 4% T/3% C stacking gels, and detected by silver staining (*31*). Initial rates of passive H^+ translocation of reconstituted proteoliposomes and DCCD-sensitive ATPase activities after binding of F_1 were determined as described (*24*).

[2] The following generalization was chosen to facilitate reading: Within the text the terms of "wildtype" (WT) and "mutant" (Mut) exclusively refer to the mutation within the S/D box of the *atpE* gene present on the corresponding plasmids.

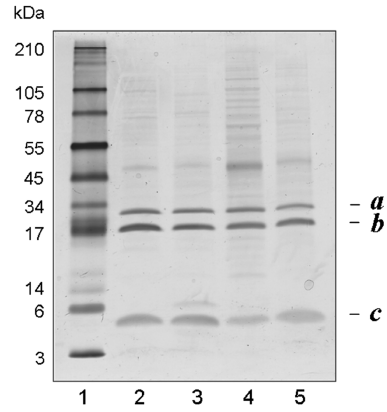

FIGURE 1: Comparison of WT-F_O and Mut-F_O preparations from strains carrying different plasmid derivatives. F_O from wildtype (WT) and mutant (Mut) strains was prepared as described in Experimental Procedures. Equimolar amounts as judged by the content of subunits *a* and *b* were separated by SDS−PAGE and silver-stained. Lane 1, molecular mass standard; lane 2, 3 μg of WT-F_O, LE392Δ*atpI-C*/pWSB30.0; lane 3, 3 μg of WT-F_O, DK8/pBWU13; lane 4, 6.5 μg of Mut-F_O, LE392Δ*atpI-C*/pRPG54; lane 5, 6.5 μg of Mut-F_O, DK8/pIA1.

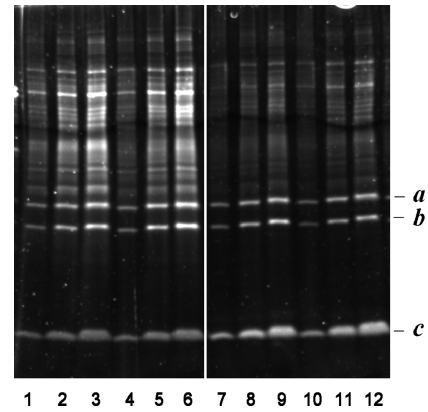

FIGURE 2: SYPRO Ruby fluorescence staining of wildtype and mutant F_O preparations after separation by SDS−PAGE. Different amounts of Mut-F_O (lanes 1−6) and WT-F_O preparations (lanes 7−12) isolated from DK8/pBWU13 and DK8/pIA1, respectively, were separated by SDS−PAGE and stained by SYPRO Ruby as described in Experimental Procedures. Two independent samples of WT-F_O and Mut-F_O were prepared in each case, and all samples were separated on the same SDS gel for precise comparative quantitation. Lanes 1 and 4, 0.8 μg of Mut-F_O; lanes 2 and 5, 1.6 μg of Mut-F_O; lanes 3 and 6, 2.4 μg of Mut-F_O; lanes 7 and 10, 0.4 μg of WT-F_O; lanes 8 and 11, 0.8 μg of WT-F_O; lanes 9 and 12, 1.2 μg of WT-F_O.

RESULTS

Densitometric Quantitation of Subunit c. F_O was prepared from *E. coli* wildtype strains DK8/pBWU13 or LE392Δ*atpI-C*/pWSB30.0 (WT-F_O) and the corresponding mutant derivatives DK8/pIA1 or LE392Δ*atpI-C*/pRPG54 (Mut-F_O). In the case of the derivatives carrying the point mutation in the S/D box, a reduced synthesis of subunit *c* was found in comparison to WT-F_O as demonstrated by SDS−PAGE (Figure 1). Staining of subunit *c* resulted in lower band intensities in the case of Mut-F_O, whereas similar band intensities were observed for subunits *a* and *b* in both WT-F_O and Mut-F_O preparations after adjustment to equimolar amounts, which means that the amount of mutant protein has been increased by a factor of 2.2 compared to wildtype (see below). Nevertheless, the F_O preparations showed comparable purity except for F_O prepared from the mutant strain LE392Δ*atpI-C*/pRPG54, a point addressed in Experimental Procedures. In order to examine the amount of subunit *c* present in wildtype and mutant, comparative densitometric analyses of F_O subunits were performed after separation of F_O preparations by SDS−PAGE and subsequent staining with SYPRO Ruby (Figure 2). The densitometric quantitation of the F_O subunits *a*, *b*, and *c* revealed that the amount of subunit *c* in Mut-F_O preparations, independent of the derivative used, is reduced by a factor of at least 2 (2.2−2.3) calculating the ratio of c_{WT}/c_{Mut} in relation to a_{WT}/a_{Mut} (Table 2). Quantitation of F_O subunits by [^{125}I]-Protein A immunolabeling, using F_O preparations from LE392Δ*atpI-C*/pWSB30.0 derivatives, also revealed an almost 2-fold (1.8) reduced amount of subunit *c* in preparations of Mut-F_O compared to WT-F_O (data not shown). This is in good accord with former studies reporting a lower expression of the mutant *atpE* gene by a factor of 2−3 (*14, 15*).

In addition, a direct comparison of the amount of subunit *a* or *b* in wildtype and mutant F_O preparations (a_{WT}/a_{Mut} or b_{WT}/b_{Mut}) revealed an overall lower synthesis of both subunits in the mutant strain (approximately a factor of 2) (Table 2), which explains the necessity of the equimolar adjustment in SDS−PAGE (Figure 1). Furthermore, DCCD-sensitive ATPase activities of membrane vesicles prepared from wildtype and mutant strains revealed a reduced activity by a factor of about 3.3 (data not shown), which is in agreement with the overall reduction of subunit *c* in wildtype and mutant F_O as determined by staining with SYPRO Ruby (c_{WT}/c_{Mut}: 4.2 ± 0.9) (Table 2). This 4-fold reduction of subunit *c* in the mutant compared to wildtype is (i) due to a general reduction of F_OF_1 synthesis by a factor of 2 (as determined by comparison of the amount of subunits *a* and *b* in mutant and wildtype) and (ii) due to an additional reduction by a factor of 2 compared to subunits *a* and *b* in mutant F_O preparations, the last point being mainly investigated in this study.

Table 2: Densitometric Quantitation of Subunits *a*, *b*, and *c* of F_O Preparations by Staining with SYPRO Ruby[a]

plasmids used (WT/Mut)	a_{WT}/a_{Mut}	b_{WT}/b_{Mut}	c_{WT}/c_{Mut}	$(c_{WT}/c_{Mut})/(a_{WT}/a_{Mut})$
pWSB30.0/pRPG54[b]	3.0 ± 0.2	4.6 ± 0.1	6.8 ± 0.4	2.3
pBWU13/pIA1[c]	1.9 ± 0.3	2.0 ± 0.2	4.2 ± 0.9	2.2

[a] Different amounts of WT-F_O and Mut-F_O preparations were separated by SDS−PAGE and stained by SYPRO Ruby as described in Experimental Procedures. The ratios of corresponding subunits of F_O from wildtype (WT) and mutant (Mut) are shown, which have been prepared from strain LE392Δ*atpI-C* bearing plasmid pWSB30.0 (WT) or plasmid pRPG54 (Mut) and of strain DK8 harboring plasmid pBWU13 (WT) or plasmid pIA1 (Mut), respectively. The reduced amount of subunit *c* in the case of Mut-F_O preparations is indicated by the *c/a* ratio. [b] Two independent data sets were taken for evaluation. [c] Three independent data sets were taken for evaluation.

Functional Analysis of Reconstituted F_O. To investigate the effects of the reduced amounts of subunit *c* on the function of F_O, reconstituted F_O was assayed for passive H^+ translocation by imposing a K^+/valinomycin diffusion potential to proteoliposomes obtained by dialysis. The resulting initial rates for H^+ uptake of Mut-F_O were significantly reduced compared to WT-F_O (2.5 and 8.6 μmol of $H^+ \cdot min^{-1} \cdot mg^{-1}$ for Mut-F_O and WT-F_O, respectively) (Figure 3) but correlated very well with the lower amount of subunit *c* present per mg of protein (Table 2). In addition,

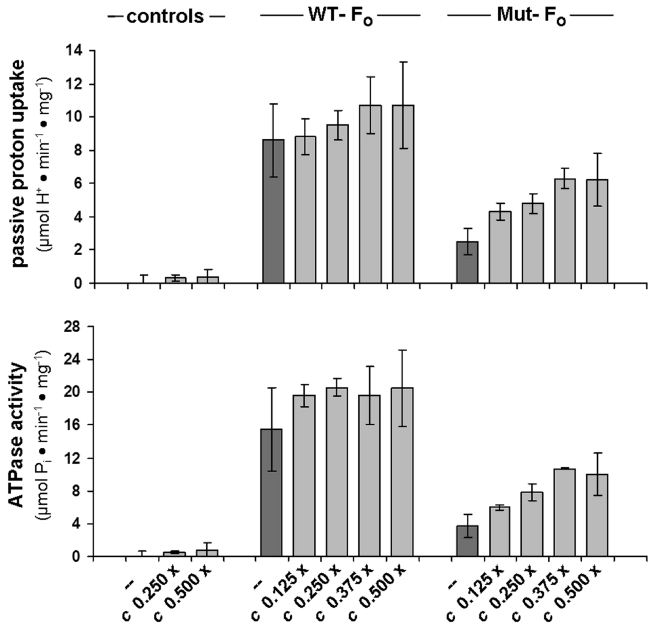

FIGURE 3: Initial rates of passive H^+ translocation of reconstituted WT-F_O and Mut-F_O preparations and coupled DCCD-sensitive ATPase activities after binding of F_1. WT-F_O and Mut-F_O were prepared from *E. coli* strain LE392Δ*atpI-C* carrying plasmids pWSB30.0 and pRPG54, respectively. Reconstitution of dialysis proteoliposomes was carried out as described in Experimental Procedures. Protein concentrations were determined by the method of Dulley and Grieve (*34*). F_O was coreconstituted with different substoichiometric multiples of detergent-dissolved subunit *c*D61 as indicated by the suffix "*x*-times". At least four independent data sets were taken for evaluation. Controls, plain liposomes, and liposomes were reconstituted only with subunit *c* (*c*D61).

after binding of F_1 to F_O-containing proteoliposomes, DCCD-sensitive coupled ATPase activity showed similar results (Figure 3). Subsequently, F_O preparations were coreconstituted with increasing substoichiometric amounts of purified wildtype subunit *c* (*c*D61). Whereas H^+ translocation rates of Mut-F_O could be successively increased by the addition of purified subunit *c*D61 by a factor of 2.5 to a value of up to 6.3 μmol of $H^+ \cdot min^{-1} \cdot mg^{-1}$, the rates of WT-$F_O$ were only slightly increased (Figure 3). The small increase in H^+ uptake of 20% for WT-F_O, was quite unexpected but can be explained by the clearing of a slight loss of subunit *c* during F_O preparation possibly due to the relative instability of the subunit *c* ring of *E. coli* compared to *c* rings of other organisms (compare refs *2, 3,* and *11*). However, the maximal rates obtained for coreconstituted Mut-F_O reached about half of the rates obtained for WT-F_O (Figure 3) as expected from the observation that the Mut-F_O preparation contained only half as much subunits *a* and *b* per mg of protein compared to WT-F_O (Table 2).

Similar results were obtained by measuring passive H^+ translocation after coreconstitution of F_O with subunit *c* by "onset solubilization" of preformed liposomes with Triton X-100 and subsequent detergent removal by treatment with Bio-Beads and use of subunit *c* purified and dissolved in chloroform/methanol/H_2O (Figure 4). Since corresponding results were obtained by use of F_O proteoliposomes coreconstituted with detergent-dissolved subunit *c* obtained by dialysis (Figure 3), this demonstrates that the results are consistent and independent of the analytical system, e.g., the reconstitution procedure and the protein-to-lipid ratio chosen for reconstitution. The uptake rates determined with the

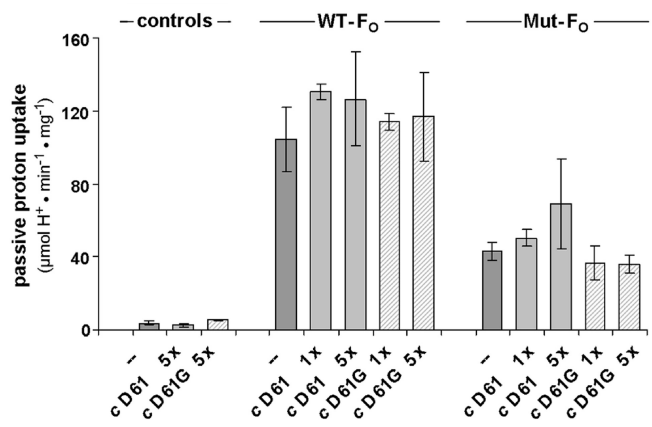

FIGURE 4: Initial rates of passive H^+ translocation of WT-F_O and Mut-F_O preparations coreconstituted with *c*D61 and *c*D61G. WT-F_O and Mut-F_O prepared from DK8/pBWU13 and DK8/pIA1, respectively, were coreconstituted with chloroform/methanol/H_2O-purified subunits *c*D61 or *c*D61G into *E. coli* phospholipid vesicles using different stoichiometric multiples of subunit *c* as indicated by the suffix "*x*-times". The protein-to-lipid ratio was 1:208 and 1:104 for WT-F_O and Mut-F_O, respectively. Protein concentrations were determined by the BCA assay. Reconstitution was performed by "onset solubilization" of preformed liposomes with Triton X-100 and detergent removal with Bio-Beads as described in Experimental Procedures. Three independent experiments were taken for evaluation. Controls, plain liposomes, and liposomes were reconstituted only with *c*D61 or *c*D61G.

second method were generally higher due to a complete removal of the detergent resulting in a bilayer tightly coupled for protons and the artificially generated potassium gradient (Figure 4). However, to achieve maximal rates of passive H^+ translocation by coreconstitution with subunit *c*, a stoichiometric excess of subunit *c* purified with chloroform/methanol/H_2O was necessary, possibly due to an incomplete refolding or an incorporation in different orientations into the lipid bilayer as has been discussed in detail by Stalz et al. (*24*). To compensate the difference in the amount of subunits *a* and *b* present in F_O preparations of wildtype and mutant, in this set of experiments Mut-F_O was reconstituted at a protein-to-lipid ratio of 1:104 instead of 1:208 for WT-F_O. As expected, proton translocation rates of Mut-F_O preparations could be increased successively upon the addition of subunit cD61 (Figure 4).

Reconstituted F_O was assayed for passive proton translocation by imposing a K^+/valinomycin diffusion potential to proteoliposomes. Contaminating proteins coreconstituted with F_O can, therefore, mask the true proton translocation rates through F_O, due to a slight leakiness of the membranes generated by impurities. For that reason, the tight coupling of the F_O proteoliposomes used for measuring the initial H^+ translocation rates was controlled directly in the same sample by its response to the uncoupler 4,5,6,7-tetrachloro-2-trifluoromethylbenzimidazole, which was always in a comparable range for the experiments described (data not shown). This indicates that the impurities have no influence on the tight coupling for protons and on the loading of the liposomes with K^+. In addition, Figure 2 shows that the amount of background impurities within the F_O preparations is the same independent of the preparation used (compare Figure 2, lanes 1 and 4 for Mut-F_O, lanes 8 and 11 for WT-F_O). Nevertheless, as a further control, the proton translocation rates measured were always tested for their sensitivity toward DCCD, a specific inhibitor of proton translocation through F_O. In each

case, a complete inhibition of the initial passive proton translocation rate was observed (data not shown), supporting that the translocation rates measured are specific for F_O.

The results obtained for Mut-F_O could on one hand be explained by a uniform population of F_O complexes comprising smaller subunit *c* rings with less monomers, which are filled up by the external addition of *c*D61. In such a homogeneous population of F_O complexes a ring size of approximately five *c* monomers would be expected due to the subunit *c* reduction by a factor of 2, thereby indicating a variable stoichiometry for the subunit *c* ring. On the other hand, the results can also be explained by a heterogeneous population concomitantly comprising fully assembled F_O complexes (ab_2c_{10}) together with free ab_2 subcomplexes. These free ab_2 subcomplexes would assemble into functional F_O complexes when externally added subunit *c* is present, thereby indicating an invariant subunit *c* stoichiometry, which is necessary for proton translocation.

After binding of F_1 to F_O proteoliposomes, DCCD-sensitive coupled ATPase activities of the mutant F_O preparation showed a comparable increase of approximately a factor of 2.7 after the addition of subunit *c*D61 during reconstitution, whereas the rates for WT-F_O were again only slightly increased for the reason already mentioned above (Figure 3). As all three F_O subunits are required for functional high-affinity binding of F_1 (*30, 36*), these results argue in favor of a heterogeneous population comprising F_O complexes as well as free ab_2 subcomplexes, because in the case of F_O complexes comprising smaller subunit *c* rings with less monomers, all three F_O subunits are present and the F_1 binding would be independent of the presence of additional subunit *c*.

In order to further discriminate between a homogeneous F_O population with smaller subunit *c* rings or the concomitant presence of fully assembled F_O together with free ab_2 subcomplexes, both Mut-F_O and WT-F_O preparations were coreconstituted with either functional *c*D61 or nonfunctional *c*D61G (Figure 4). *c*D61G is missing the essential carboxylate in the middle of the C-terminal transmembrane helix involved in H^+ translocation (*37*) and has already been shown to produce inactive F_O complexes, if incorporated into subunit *c*D61 rings built up *de novo* from single subunits (*27*). In this context it is noteworthy to mention that the presence of one copy of *c*D61G within the oligomer is sufficient to block H^+ translocation completely (*27*). Whereas the proton uptake rates of Mut-F_O were increased by coreconstitution with increasing amounts of subunit *c*D61 as described above, the addition of different amounts of nonfunctional *c*D61G affected neither the proton translocation of WT-F_O nor that of Mut-F_O (Figure 4). Since it was expected that incorporation of *c*D61G into subunit *c* rings leads to the inactivation of proton translocation, these results clearly demonstrate that externally added subunit *c*, either *c*D61 or *c*D61G, did not incorporate into assembled subunit *c* rings. Otherwise, translocation rates should have significantly dropped in the presence of *c*D61G. Furthermore, also the translocation rates of Mut-F_O remained unaltered with *c*D61G, which clearly indicates that in Mut-F_O preparations inactive F_O complexes were assembled *de novo* from a fraction of ab_2 subcomplexes and externally added *c*D61G, whereas in the presence of wildtype *c*D61 active F_O complexes were assembled *de novo*, resulting in an increase in proton translocation as observed.

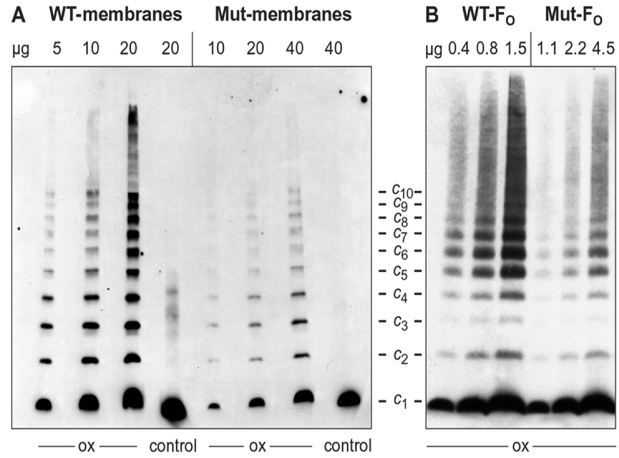

FIGURE 5: Immunoblot analysis of cross-linked subunit *c* (*c*A21C/*c*M65C) in membrane vesicles and proteoliposomes of wildtype and mutant. Membranes prepared from DK8/pBWU13.NOC and DK8/pIA1.NOC as well as proteoliposomes containing bicysteine-substituted WT-F_O and Mut-F_O, respectively, were separated after cross-linking by nonreducing SDS−PAGE and immunoblotted. Detection of bands containing subunit *c* was performed using the mAb GDH 9-2A2. (A) Copper-1,10-phenanthroline-catalyzed cross-linking of subunit *c* with bicysteine substitutions (*c*A21C/*c*M65C) in membrane vesicles of wildtype and mutant. (B) Cross-linking of subunit *c* (*c*A21C/*c*M65C) in proteoliposomes containing WT-F_O or Mut-F_O catalyzed by air oxidation. In general, the amount of individual subunit *c* oligomer intermediates varied from experiment to experiment (e.g., the almost complete absence of the c_3 oligomer in reconstituted liposomes is such a single observation in the experiment shown) but was always comparable for wildtype and mutant. ox, oxidized sample; control, addition of 50 mM EDTA and 25 mM *N*-ethylmaleimide prior to oxidation.

Investigation of Subunit c Stoichiometry by Cross-Link Analyses. The results obtained from the functional analyses of reconstituted F_O implicated a heterogeneous Mut-F_O population consisting of fully assembled F_O complexes (ab_2c_{10}) and free ab_2 subcomplexes. In order to analyze the structural phenotype of the mutant with respect to subunit *c* stoichiometry, membrane vesicles of the wildtype and mutant strain carrying plasmids, which additionally encode the bicysteine substitution *c*A21C/*c*M65C, were prepared. Intermolecular cross-links were generated with copper-1,10-phenanthroline according to Jones et al. (*32*) and analyzed by immunoblotting (Figure 5A). Formation of an identical cross-linking pattern for subunit *c* in both wildtype and mutant membranes could be observed, which strongly argues in favor of a comparable subunit *c* stoichiometry with ten *c* monomers per ring in both F_OF_1 complexes at least on the level of membrane vesicles. However, due to an incomplete cross-linking of the subunit *c* ring (10 cross-link events are expected to occur at most; compare refs *12, 13,* and *32*), all other intermediates of subunit *c* oligomerization are also visible in appreciable amounts stopping at the level of decamer formation, thereby generating a ladder-like appearance (Figure 5). It should be emphasized at this point that from these results it cannot be concluded that all of the oligomers have exactly the same number. In addition, the results obtained by activity measurements and cross-linking experiments do not have the precision to detect an eventually occurring difference of 1 or 2 in stoichiometry. However, the determination of the exact number of *c* subunits within the ring is not the intention of this study. Furthermore, the lack of precision of the technique is not only valid for the

wildtype and mutant subunit *c* stoichiometry in this study but does also apply to the data obtained by Bob Fillingame's group (*12*, *13*, *32*) leading to the conclusion that the preferred number of *c* subunits per ring is 10. Nevertheless, in the case of smaller *c* rings within Mut-F_O, the ladder-like bands of subunit *c* oligomers would stop approximately at the level of pentamer formation due to the reduced amount of subunit *c* monomers present per ring, which would readily be detectable with the technique used in this study but was not observed during the experiments. On the contrary, to obtain comparable intensities for the bands analyzed by immunoblotting, the amount of mutant membrane protein had to be increased to compensate for the reduction of subunit *c* synthesis in the mutant strain, especially in the presence of additional cysteine residues in the transmembrane helices. The need for an equimolar adjustment also underlines that the number of *c* subunits in the rings does not change in dependence on the amount of subunit *c* produced. The faint bands observed above the decamer level are inherent in using membrane vesicles and were also found in corresponding studies of R. H. Fillingame's group (*12, 13, 32*). By purification of F_OF_1 after cross-linking, Jiang et al. (*13*) showed that these products appear to be minor artifacts of assembly formed in the membrane, which do not represent functional F_OF_1 complex.

In order to show whether this also applies for reconstituted F_O, a corresponding cross-link analysis catalyzed by air oxidation was also performed with bicysteine-substituted WT-F_O and Mut-F_O preparations reconstituted in liposomes (Figure 5B). Although the higher oligomeric products, especially nonamer and decamer of subunit *c*, could not be resolved very well in SDS−PAGE possibly due to lipid interference, the pattern of cross-linked subunit *c* was again found to be identical in either case (Figure 5B), thereby underlining a fixed subunit *c* stoichiometry within the assembled F_O complexes of both wildtype and mutant and the absence of smaller *c* rings due to the reduction of subunit *c* synthesis.

Finally, to verify the presence of free ab_2 subcomplexes in the mutant strain, further cross-linking experiments were performed using the double cysteine substitution *a*N214C/*c*M65C, which has already been demonstrated to cross-link subunits *a* and *c* with an efficiency of 40% using copper-1,10-phenanthroline (*21*) or almost 100% in the case of iodine-catalyzed cross-linking (*29*). In our study, cross-linking of membrane vesicles of both wildtype and mutant strains, also containing the double cysteine substitution *a*N214C/*c*M65C, was carried out by air oxidation according to McLachlin and Dunn (*34*) and detected by immunoblotting. Under these conditions cross-link formation occurred with an efficiency of 80−100% for subunit *a*. Figure 6 shows a representative immunoblot in combination with a cumulative column diagram of quantitated band signals. In order to achieve a linear range of band signal intensities, blot development was stopped when the strongest signal reached its saturating intensity (Figure 6A). Under these conditions, cross-link formation in wildtype membranes was almost 100% for subunit *a* as expected, whereas in the case of Mut-F_O preparations a cross-link yield of only about 50% could be achieved for subunit *a* (Figure 6B). This clearly demonstrates the presence of free ab_2 subcomplexes within Mut-F_O preparations, which could naturally not be cross-linked

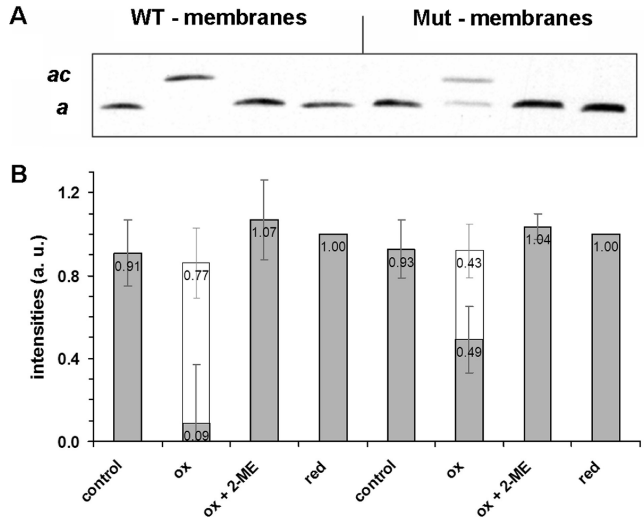

FIGURE 6: Identification of free ab_2 subcomplexes in Mut-F_O. Membranes of wildtype and mutant with double cysteine substitution *a*N214C/*c*M65C were reduced by DTT prior to cross-linking, which was induced by air oxidation in the presence of 50 μM $CuCl_2$. 10 and 27 μg of membrane vesicles of wildtype and mutant, respectively, were subjected to nonreducing SDS−PAGE and immunoblotted in order to compensate for the difference in the amount of total F_O complexes present in the membranes. Detection of bands containing subunit *a* was performed by use of the mAb GDH 8-8B3 as described in Experimental Procedures. (A) Immunoblotting of membrane vesicles of wildtype and mutant. Since no other bands were detected on the immunoblot membrane with subunit *a*-specific antibodies, only the section of interest is presented. Control, untreated sample; ox, oxidized sample; ox + 2-ME, addition of 143 mM 2-ME after oxidation; red, DTT-reduced sample immediately taken prior to oxidation. (B) Averaged densitometric quantitation of signal intensities. Signal intensities of the DTT-reduced samples were set to 1. Three independent cross-link experiments were taken for evaluation. White bars, signal intensities of the *ac* cross-link product; gray bars, signal intensities of subunit *a*. a.u., arbitrary units.

to subunit *c*, and is in good accord with the results obtained by passive H^+ translocation and DCCD-sensitive ATPase activity measurements as well as the densitometric quantitations of F_O subunits.

DISCUSSION

It is generally accepted that subunit *c* assembles into oligomeric ring-like structures within the F_O complex. Structural data on subunit *c* oligomers demonstrate that the stoichiometry varies between 10 and 15 among different organisms (*3*, *6*−*9*). The number of *c* subunits present in each ring indicates the number of protons/ions transported across the membrane during each cycle of the ATP synthase. As a consequence, due to the three catalytic sites present in F_1 and a synthesis rate of three molecules of ATP per cycle, a variation in the number of *c* subunits and, therefore, proton/ion binding sites in the *c* ring of different species automatically leads to different proton/ion to ATP ratios ranging from 3.3 to 5 per ATP synthesized. ATP synthases with large *c* rings have high ratios, which seems to be advantageous for the cell's ATP synthesis at low proton/ion motive force. On the contrary, ATP synthases with small *c* rings might predominate in species with constantly high proton/ion motive force resulting in a more efficient use of energy. In the case of *E. coli* ATP synthase, subunit *c* stoichiometry was assumed to be preferentially 10 (*13*), which was derived

from cross-linking experiments. Additionally, oligomers of *E. coli* subunit *c* generated by genetic fusion (*12, 13*), which exhibited functional *c* rings consisting of up to 12 monomers, enforced the discussion about a possible stoichiometric variability. However, oligomeric cross-link products migrating at molecular masses above c_{10} were not observed in purified F_OF_1 (*13*) and appear to be artifacts of assembly formed in the membrane, which do not represent functional F_OF_1 complex. In contrast, corresponding experiments with genetically fused subunit *c* multimers of thermophilic *Bacillus* PS3 ATP synthase revealed that the *c* ring of this organism is a decamer (*38*). However, the controversially discussed issue of subunit *c* stoichiometry of *E. coli* ATP synthase is inevitably associated with the ratio of H^+/ATP during ATP hydrolysis/synthesis and, hence, the P/O ratio of oxidative phosphorylation. Based on current models (*5, 39*), the H^+/ATP ratio as well as the direction of ATP hydrolysis or synthesis could be adjusted by the subunit *c* stoichiometry, thereby maintaining an efficient energy conversion, if the stoichiometry is regulated depending on external influences like the metabolic status of the cell (*14*). Whereas Schemidt and co-workers suggested a regulated and, therefore, variable subunit *c* stoichiometry dependent on the carbon source provided for cell growth (*14*), a constrained and fixed stoichiometry is implicated by the finding of open subunit *c* rings in the case of chloroplasts and *I. tartaricus* as observed by atomic force microscopy (*11*) and by the self-assembly of detergent-dissolved subunit *c* of *E. coli* into rings (*40*). This argues in favor of the notion that the amino acid sequence and, therefore, the biochemical properties of the monomer invariantly determine the shape and size of the proteolipid ring. In addition, studies on the chloroplast subunit *c* oligomer of the algae *Chlamydomonas reinhardtii* revealed a fixed stoichiometry that is not affected by the metabolic status of the cell, caused by variations in light intensity, pH value, carbon source, or CO_2 concentration (*41*).

In a previous study (*18*), immunoblot quantitations of subunits *b* and *c* in F_OF_1 preparations isolated from wildtype and mutant cells revealed a reduction in synthesis of subunit *c* due to a point mutation in the S/D box of the corresponding *atpE* gene. These findings suggested the presence of subunit *c* rings reduced in size and, therefore, a variable stoichiometry of subunit *c*. Studies on the *c* ring of the mutant strain and its stoichiometry now revealed a detailed picture: Rates of passive H^+ translocation of reconstituted F_O strongly correlated with the amount of subunit *c* present, which was quantitated after staining of F_O subunits in SDS gels with SYPRO Ruby. Mut-F_O preparations showed significantly lower translocation rates upon reconstitution than WT-F_O, and the H^+ translocation rate of the Mut-F_O preparation could be increased by the addition of purified subunit *c*D61 during reconstitution. However, the same could be observed for the DCCD-sensitive coupled ATPase activity of reconstituted F_O after binding of F_1. Whereas the H^+ translocation activities apparently argue in favor of a possible variable subunit *c* stoichiometry at least *in vitro*, the analyses of ATPase activities contradict this conclusion. For functional binding of F_1, all three F_O subunits are necessary (*30, 36*), although only four to five monomers of the subunit *c* oligomer are directly involved in F_1 interaction (*42*). A status that is also realized in the case of F_O complexes comprising *c* rings with less monomers, therefore, expecting the binding of F_1 to be independent of the presence of additional subunit *c*. Furthermore, the results obtained from coreconstitution of F_O with inactive *c*D61G clearly support the concomitant presence of fully assembled F_O complexes and free ab_2 subcomplexes in the case of the mutant. Titration of *c*D61G did not affect the H^+ translocation rates of both the wildtype and the mutant, whereas the H^+ translocation could be increased by the addition of *c*D61, suggesting free ab_2 subcomplexes, which were assembled to functional F_O complexes. A dissociation of the subunit *c* ring during reconstitution can be excluded, because the *de novo* assembly of F_O from single subunits in the presence of *c*D61G leads to the formation of inactive complexes (*27*). In addition, the reconstitution of purified ab_2 subcomplexes to functional F_O complexes in the presence of subunit *c* has previously been demonstrated (*24*).

The results obtained from the measurements of passive H^+ translocation and ATPase activity are further supplemented by intermolecular cross-linking performed by use of the bicysteine substitution *c*A21C/*c*M65C, which was previously used to determine that the stoichiometry of subunit *c* is preferred to be 10 (*13*). Using the same method to compare the stoichiometry of subunit *c* of both wildtype and mutant, our data revealed that comparable subunit *c* oligomers were formed in both cases, although the amount of subunit *c* present in mutant membranes was reduced. Although the absolute number of *c* subunits cannot be derived from these kinds of experiments as has already been discussed by Jiang et al. (*13*), we are also favoring a stoichiometry of 10 in either case. Nevertheless, the comparable pattern in oligomerization for wildtype and mutant excluded the possibility that the massive reduction in subunit *c* synthesis leads to the formation of smaller *c* rings with four to six *c* subunits per ring. Furthermore, the heterogeneous character of Mut-F_O preparations, consisting of fully assembled F_O complexes and free ab_2 subcomplexes, was clearly demonstrated by cross-linking of *a*N214C to *c*M65C in membrane vesicles. The reduced synthesis of subunit *c* compared to subunits *a* and *b* could be confirmed by a cross-link yield of only 50% with respect to subunit *a* in the case of mutant F_O preparations, whereas the cross-link formation in wildtype F_O was almost 100%. In the case of the mutant, these findings fit very well with a concomitant presence of fully assembled F_O complexes and free ab_2 subcomplexes in a 1:1 ratio and are in good agreement with a reduction of subunit *c* by a factor of 2 compared to subunits *a* and *b*.

The insertion of *in vitro* synthesized subunit *c* into proteoliposomes in its native transmembrane topology is catalyzed by the membrane protein insertase YidC, whereupon subunit *c* assembles into oligomers with a molecular mass of approximately 80−100 kDa (*43, 44*). In addition, purified subunit *c* dissolved in detergent solution showed a self-assembly into rings (*40*). Hence, as discussed previously (*40*), it is likely that the unique biochemical properties of the proteolipid based on its primary structure determine the shape and size of the ring, resulting in an invariability of the subunit *c* stoichiometry on the level of assembly. Based on the visualization of purified subunit *c* oligomers from spinach chloroplasts and *I. tartaricus* ATP synthase by AFM, the stoichiometry and diameter of the *c* oligomer may be conceivably constrained by the shape of the subunits and their nearest neighbor interactions, even for open *c* rings, in which some of the *c* subunits are missing (*11*). The subunit

c ring of *I. tartaricus* is thought to be stabilized by the binding of the Na^+ coupling ion (*45, 46*) and, hence, resembles a rather rigid structure. The structure of the *c* oligomer of *E. coli* is less stable and, though, can be assumed to be more flexible, since genetically fused multimers of subunit *c* yielded functional proteolipid rings with an artificial stoichiometry ranging from 9 to 12 (*12, 13*). Although the stoichiometry of subunit *c* in *E. coli* can thus be forced to deviate to a certain extent, the preferred stoichiometry was revealed to be 10 (*13*). A similar approach was performed with subunit *c* of the thermophilic *Bacillus* PS3 ATP synthase, comprising fused proteolipids consisting of up to 14 monomers (*38*). In contrast to *E. coli*, only F_OF_1 containing decameric subunit *c* rings, combined from c_1-, c_2-, c_5-, or c_{10}-fused multimers, exhibited a functional phenotype, thereby indicating a comparatively less structural flexibility as could be expected for a thermostable enzyme.

Taken together, these data clearly demonstrate an identical stoichiometry of subunit *c* in *E. coli* ATP synthase in the case of the mutant strain carrying a G → A base transition within the S/D box of the *atpE* gene compared to wildtype. Hence, the previous postulate of an altered stoichiometry of the subunit *c* ring in dependence on the expression level of the *atpE* gene (*18*) is no longer valid. Even if the cell is genetically forced to produce substoichiometric amounts of subunit *c*, a heterogeneous population comprising F_O complexes with wildtype subunit *c* oligomers and ab_2 subcomplexes free of subunit *c* is the consequence instead of the formation of smaller proteolipid rings. Therefore, these findings exclude a dynamic subunit *c* stoichiometry as a regulatory mechanism, at least on the level of protein synthesis.

ACKNOWLEDGMENT

Drs. O. Y. Dmitriev and R. H. Fillingame (University of Wisconsin Medical School, Madison, WI) are kindly acknowledged for generously providing strains and plasmids.

REFERENCES

1. Weber, J., and Senior, A. E. (2003) ATP synthesis driven by proton transport in F_1F_O-ATP synthase. *FEBS Lett. 545*, 61–70.
2. Fillingame, R. H., Angevine, C. M., and Dmitriev, O. Y. (2003) Mechanics of coupling proton movements to c-ring rotation in ATP synthase. *FEBS Lett. 555*, 29–34.
3. Dimroth, P., von Ballmoos, C., and Meier, T. (2006) Catalytic and mechanical cycles in F-ATP synthases. *EMBO Rep. 7*, 276–282.
4. Kinosita, K., Jr., Adachi, K., and Itoh, H. (2004) Rotation of F_1-ATPase: How an ATP-driven molecular machine may work. *Annu. Rev. Biophys. Biomol. Struct. 33*, 245–268.
5. Junge, W., and Nelson, N. (2005) Nature's rotary electromotors. *Science 308*, 642–644.
6. Meier, T., Ferguson, S. A., Cook, G. M., Dimroth, P., and Vonck, J. (2006) Structural investigations of the membrane-embedded rotor ring of the F-ATPase from *Clostridium paradoxum*. *J. Bacteriol. 188*, 7759–7764.
7. Toei, M., Gerle, C., Nakano, M., Tani, K., Gyobu, N., Tamakoshi, M., Sone, N., Yoshida, M., Fujiyoshi, Y., Mitsuoka, K., and Yokoyama, K. (2007) Dodecamer rotor ring defines H^+/ATP ratio for ATP synthesis of prokaryotic V-ATPase from *Thermus thermophilus*. *Proc. Natl. Acad. Sci. U.S.A. 104*, 20256–20261.
8. Pogoryelov, D., Reichen, C., Klyszejko, A. L., Brunisholz, R., Müller, D. J., Dimroth, P., and Meier, T. (2007) The oligomeric state of c rings from cyanobacterial F-ATP synthases varies from 13 to 15. *J. Bacteriol. 189*, 5895–5902.
9. Lolkema, J. S., and Boekema, E. J. (2003) The A-type ATP synthase subunit K of *Methanopyrus kandleri* is deduced from its sequence to form a monomeric rotor comprising 13 hairpin domains. *FEBS Lett. 543*, 47–50.
10. Meier, T., Yu, J., Raschle, T., Henzen, F., Dimroth, P., and Müller, D. J. (2005) Structural evidence for a constant c_{11} ring stoichiometry in the sodium F-ATP synthase. *FEBS J. 272*, 5474–5483.
11. Müller, D. J., Dencher, N. A., Meier, T., Dimroth, P., Suda, K., Stahlberg, H., Engel, A., Seelert, H., and Matthey, U. (2001) ATP synthase: Constrained stoichiometry of the transmembrane rotor. *FEBS Lett. 504*, 219–222.
12. Jones, P. C., and Fillingame, R. H. (1998) Genetic fusions of subunit *c* in the F_O sector of H^+-transporting ATP synthase. Functional dimers and trimers and determination of stoichiometry by cross-linking analysis. *J. Biol. Chem. 273*, 29701–29705.
13. Jiang, W., Hermolin, J., and Fillingame, R. H. (2001) The preferred stoichiometry of *c* subunits in the rotary motor sector of *Escherichia coli* ATP synthase is 10. *Proc. Natl. Acad. Sci. U.S.A. 98*, 4966–4971.
14. Schemidt, R. A., Qu, J., Williams, J. R., and Brusilow, W. S. A. (1998) Effects of carbon source on expression of F_O genes and on the stoichiometry of the *c* subunit in the F_1F_O ATPase of *Escherichia coli*. *J. Bacteriol. 180*, 3205–3208.
15. Tomashek, J. J., and Brusilow, W. S. A. (2000) Stoichiometry of energy coupling by proton-translocating ATPases: A history of variability. *J. Biomembr. Bioenerg. 32*, 493–500.
16. Schaefer, E. M., Hartz, D., Gold, L., and Simoni, R. D. (1989) Ribosome-binding sites and RNA-processing sites in the transcript of the *Escherichia coli unc* operon. *J. Bacteriol. 171*, 3901–3908.
17. Solomon, K. A., and Brusilow, W. S. A. (1988) Effect of an *uncE* ribosome-binding site mutation on the synthesis and assembly of the *Escherichia coli* proton-translocating ATPase. *J. Biol. Chem. 263*, 5402–5407.
18. Schemidt, R. A., Hsu, D. K. W., Deckers-Hebestreit, G., Altendorf, K., and Brusilow, W. S. A. (1995) The effects of an *atpE* ribosome-binding site mutation on the stoichiometry of the c subunit in the F_1F_O ATPase of *Escherichia coli*. *Arch. Biochem. Biophys. 323*, 423–428.
19. Gunsalus, R. P., Brusilow, W. S. A., and Simoni, R. D. (1982) Gene order and gene-polypeptide relationships of the proton-translocating ATPase operon (*unc*) of *Escherichia coli*. *Proc. Natl. Acad. Sci. U.S.A. 79*, 320–324.
20. Moriyama, Y., Iwamoto, A., Hanada, H., Maeda, M., and Futai, M. (1991) One-step purification of *Escherichia coli* H^+-ATPase (F_OF_1) and its reconstitution into liposomes with neurotransmitter transporters. *J. Biol. Chem. 266*, 22141–22146.
21. Jiang, W., and Fillingame, R. H. (1998) Interacting helical faces of subunits *a* and *c* in the F_1F_O ATP synthase of *Escherichia coli* defined by disulfide cross-linking. *Proc. Natl. Acad. Sci. U.S.A. 95*, 6607–6612.
22. Fraga, D., Hermolin, J., Oldenburg, M., Miller, M. J., and Fillingame, R. H. (1994) Arginine 41 of subunit *c* of *Escherichia coli* H^+-ATP synthase is essential in binding and coupling of F_1 to F_O. *J. Biol. Chem. 269*, 7532–7537.
23. Klionsky, D. J., Brusilow, W. S. A., and Simoni, R. D. (1984) In vivo evidence for the role of the ϵ subunit as an inhibitor of the proton-translocating ATPase of *Escherichia coli*. *J. Bacteriol. 160*, 1055–1060.
24. Stalz, W.-D., Greie, J.-C., Deckers-Hebestreit, G., and Altendorf, K. (2003) Direct interaction of subunits *a* and *b* of the F_O complex of *Escherichia coli* ATP synthase by forming an ab_2 subcomplex. *J. Biol. Chem. 278*, 27068–27071.
25. Angov, E., and Brusilow, W. S. A. (1988) Use of *lac* fusions to measure in vivo regulation of expression of *Escherichia coli* proton-translocating ATPase (*unc*) genes. *J. Bacteriol. 170*, 459–462.
26. Brusilow, W. S. A. (1987) Proton leakiness caused by cloned genes for the F_O sector of the proton-translocating ATPase of *Escherichia coli*: Requirement for F_1 genes. *J. Bacteriol. 169*, 4984–4990.
27. Dmitriev, O. Y., Altendorf, K., and Fillingame, R. H. (1995) Reconstitution of the F_O complex of *Escherichia coli* ATP synthase from isolated subunits. Varying the number of essential carboxylates by co-incorporation of wild-type and mutant subunit *c* after purification in organic solvent. *Eur. J. Biochem. 233*, 478–483.
28. Birkenhäger, R., Greie, J.-C., Altendorf, K., and Deckers-Hebestreit, G. (1999) F_O complex of the *Escherichia coli* ATP synthase. Not all monomers of the subunit *c* oligomer are involved in F_1 interaction. *Eur. J. Biochem. 264*, 385–396.
29. Hutcheon, M. L., Duncan, T. M., Ngai, H., and Cross, R. L. (2001) Energy-driven subunit rotation at the interface between subunit *a* and the *c* oligomer in the F_O sector of *Escherichia coli* ATP synthase. *Proc. Natl. Acad. Sci. U.S.A. 98*, 8519–8524.

30. Schneider, E., and Altendorf, K. (1985) All three subunits are required for the reconstitution of an active proton channel (F_O) of *Escherichia coli* ATP synthase (F_1F_O). *EMBO J. 4*, 515–518.
31. Greie, J.-C., Deckers-Hebestreit, G., and Altendorf, K. (2000) Secondary structure composition of reconstituted subunit *b* of the *Escherichia coli* ATP synthase. *Eur. J. Biochem. 267*, 3040–3048.
32. Jones, P. C., Jiang, W., and Fillingame, R. H. (1998) Arrangement of the multicopy H^+-translocating subunit *c* in the membrane sector of the *Escherichia coli* F_1F_O ATP synthase. *J. Biol. Chem. 273*, 17178–17185.
33. Douglas, M., Finkelstein, D., and Butow, R. A. (1979) Analysis of products of mitochondrial protein synthesis in yeast: Genetic and biochemical aspects. *Methods Enzymol. 56*, 58–66.
34. McLachlin, D. T., and Dunn, S. D. (1997) Dimerization interactions of the *b* subunit of the *Escherichia coli* F_1F_O-ATPase. *J. Biol. Chem. 272*, 21233–21239.
35. Dulley, J. R., and Grieve, P. A. (1975) A simple technique for eliminating interference by detergents in the Lowry method of protein determination. *Anal. Biochem. 64*, 136–141.
36. Krebstakies, T., Zimmermann, B., Gräber, P., Altendorf, K., Börsch, M., and Greie, J.-C. (2005) Both rotor and stator subunits are necessary for efficient binding of F_1 to F_O in functionally assembled *Escherichia coli* ATP synthase. *J. Biol. Chem. 280*, 33338–33345.
37. Fillingame, R. H., Peters, L. K., White, L. K., Mosher, M. E., and Paule, C. R. (1984) Mutations altering aspartyl-61 of the omega subunit (*uncE* protein) of *Escherichia coli* H^+-ATPase differ in effect on coupled ATP hydrolysis. *J. Bacteriol. 158*, 1078–1083.
38. Mitome, N., Suzuki, T., Hayashi, S., and Yoshida, M. (2004) Thermophilic ATP synthase has a decamer *c*-ring: Indication of noninteger 10:3 H^+/ATP ratio and permissive elastic coupling. *Proc. Natl. Acad. Sci. U.S.A. 101*, 12159–12164.
39. Dimroth, P., von Ballmoos, C., Meier, T., and Kaim, G. (2003) Electrical power fuels rotary ATP synthase. *Structure (Cambridge) 11*, 1469–1473.
40. Arechaga, I., Butler, P. J. G., and Walker, J. E. (2002) Self-assembly of ATP synthase subunit c rings. *FEBS Lett. 515*, 189–193.
41. Meyer zu Tittingdorf, J. M. W., Rexroth, S., Schäfer, E., Schlichting, R., Giersch, C., Dencher, N. A., and Seelert, H. (2004) The stoichiometry of the chloroplast ATP synthase oligomer III in *Chlamydomonas reinhardtii* is not affected by the metabolic state. *Biochim. Biophys. Acta 1659*, 92–99.
42. Watts, S. D., and Capaldi, R. D. (1997) Interactions between the F_1 and F_O parts in the *Escherichia coli* ATP synthase. Associations involving the loop region of *c* subunits. *J. Biol. Chem. 272*, 15065–15068.
43. van der Laan, M., Bechtluft, P., Kol, S., Nouwen, N., and Driessen, A. J. M. (2004) F_1F_O ATP synthase subunit c is a substrate of the novel YidC pathway for membrane protein biogenesis. *J. Cell. Biol. 165*, 213–222.
44. Kol, S., Turrell, B. R., de Keyzer, J., van der Laan, M., Nouwen, N., and Driessen, A. J. M. (2006) YidC-mediated membrane insertion of assembly mutants of subunit c of the F_1F_O ATPase. *J. Biol. Chem. 281*, 29762–29768.
45. Meier, T., Polzer, P., Diederichs, K., Welte, W., and Dimroth, P. (2005) Structure of the rotor ring of F-type Na^+-ATPase from *Ilyobacter tartaricus*. *Science 308*, 659–662.
46. Meier, T., and Dimroth, P. (2002) Intersubunit bridging by Na^+ ions as a rationale for the unusual stability of the c-rings of Na^+-translocating F_1F_O ATP synthases. *EMBO Rep. 3*, 1094–1098.

BI800173A